Influence of CaO or CeO_2 coatings on oxidation of nickel polycrystals.

N.Halem, Z.Halem, M.Abrudeanu**,S.Chekroud***, G.Petot-Ervas*****

Elaboration and characterization of Materials, University Mouloud Mammeri, 15000 Tizi Ouzou, Algeria

** University of Bouira, Algeria*

***University of Pitesti, LSIM, Romania*

*****Constantine University, Campus Ersas, Algeria*

*****Research group CNRS/SPMS/ECP/92 Châtenay Malabry & CEA Saclay, 91 Gif sur Yvette (France)*

Corresponding author : G.Petot Ervas, georgette.petot@yahoo.fr

Summary

The present study is concerned with the influence of CaO, or CeO_2, sputter coatings on the oxidation behavior of specpure Ni polycrystals. The experiments were performed between 800° and 1200°C. The CeO_2-coated specimens show a more pronounced decrease of the oxidation kinetics than those coated with CaO. The beneficial influence of these coatings is first explained by the presence of CaO, or CeO_2 precipitates near the position of the initial metal surface. For the CeO_2-coated specimens, the lower oxidation rates are also due to the decrease of the vacancy diffusion coefficient, while for the CaO coatings, it results of the decrease of the driving force of diffusion, due to the shift of the Ni/NiO phase boundary to higher P_{O2}.

1 Introduction

In the present investigation we have studied the oxidation of CaO, or CeO_2-coated nickel polycrystals. Coatings were produced by sputtering a CaO, or CeO_2, target directly on polycrystalline Ni coupons [1]. Thermogravimetric analysis and structural characterizations were performed to study their effect on both nickel oxidation kinetics and oxide layer morphologies [1,2] These results have been analysed taking into account, both thermodynamic and transport properties of undoped and Ca (or Ce)-doped $Ni_{1-x}0$ single crystals and a fundamental analysis of transport processes under non equilibrium conditions.

2 Materials and methods

The specimens were nickel oxidized square coupons (1 cm^2 by 0.1 cm thick) prepared from high purity powders (99.995 wt %), sintered at 1200°C, under Ar/H_2 mixtures.[1,2]. The oxide scale was removed on one main surface (1cm^2). This face was slightly polished to a 1μm diamond finish and coated by sputtering a CaO or CeO_2 target in an ambient of

7×10^{-2} mbar argon, during one hour [1]. Oxidation experiments were carried out at temperatures between 800° and 1200°C, in a Setaram thermobalance [1,2]. The microstructure of the oxide scales was examined by scanning electron microscopy (SEM) and the composition was evaluated by EPMA analysis [1].

3 Influence of coatings on nickel oxidation

3.1 Oxidation kinetics

The oxidation kinetic curves for uncoated and CaO, or CeO_2-coated polycrystalline nickel coupons are reported in Fig.1-3, from 800° to 1200°C, in air. They show that CeO_2 coatings lead to a more pronounced decrease of oxidation kinetics than CaO coatings (Fig.2). In agreement with Wagner theory [3], the results follow a parabolic law. Diffusion processes through oxidation scale are then rate determining and weight gain per unit area (Δm/s) can be expressed by::

$$(\Delta m/s) = k_p \sqrt{t} + k_o \qquad (1)$$

where kp is the parabolic rate constant.

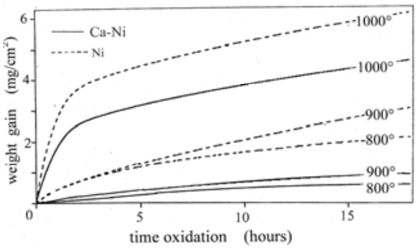

Figure.1 Weight gain of uncoated and CaO-coated Ni

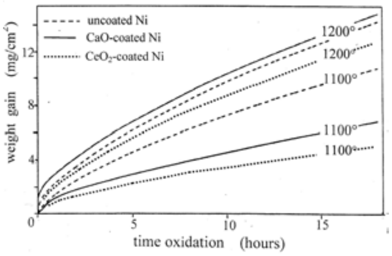

Figure.2 CaO and CeO_2-coated Ni

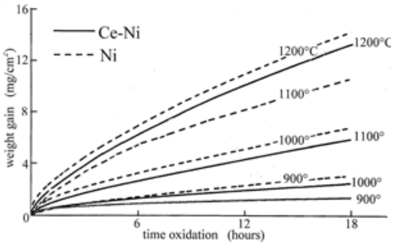

Figure 3 Weight gain of uncoated and CeO_2-coated Ni

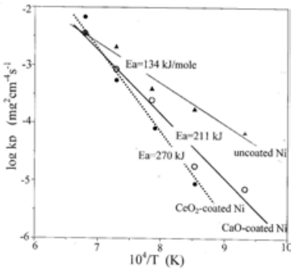

Figure 4 Arrhenius plot of kp

The Arrhenius plots of kp are reported in Fig.4. The activation energies (Ea) show a reasonable agreement with the Ni grain boundary diffusion activation energy in $Ni_{1-x}O$ (Ea=172 kJ [4]), despite the less precise values of E_a(kp), due to grain size changes with time and through the oxide layer.

3.2 Morphology of scales

The oxide surfaces are characterized by the facetted morphology observed in cationic growing scales [1,2,3]. Typical micrographs (Fig 5) illustrate fracture sections of oxide layers developed on coated and uncoated nickel polycrystals, oxidized at 1100°C. As observed in previous nickel oxidation works [1,2,3], the oxide films have a duplex structure and the inner/outer layer boundary coincides likely with the position of the original metal surface, as suggested in earlier works [4]. In contrast to uncoated nickel (Fig.5a), no crack is seen at the metal/oxide interface of the coated specimens (Fig.5b,c).

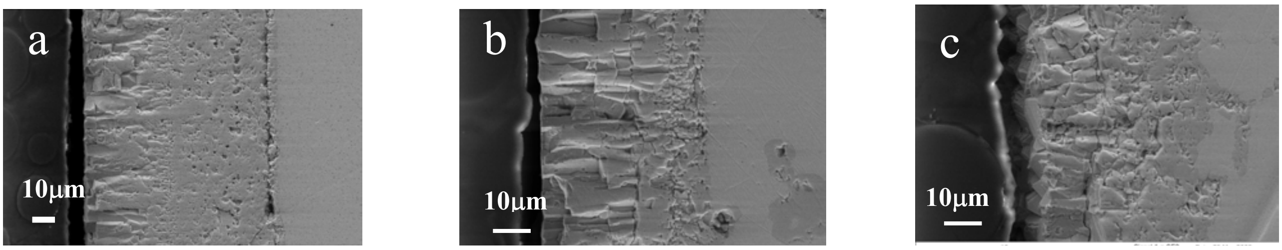

Figure.5 Cross section of (a) uncoated and (b) CaO or (c) CeO_2–coated nickel, oxidized at 1100°C.

3.3 *Composition of scales*

The calcium and cerium depth profiles through the oxide layers formed on coated specimens were investigated by EPMA analysis [1]. At 900°C, a high concentration of Ca^{2+} or Ce^{4+} is observed in a localized zone, which coincides likely with the position of the original metal surface, i.e. with the inner/outer layer boundary. It should be noted, that from either side of this maximum, the amount of Ca^{2+} is higher in the outer layer, while the amount of Ce^{4+} is higher in the inner layer. According to the outward diffusion of cationic species in the growing oxide scales, it follows that in $Ni_{1-x}0$:

$$D_{Ca}>D_{Ni}>D_{Ce}. \qquad * \tag{2}$$

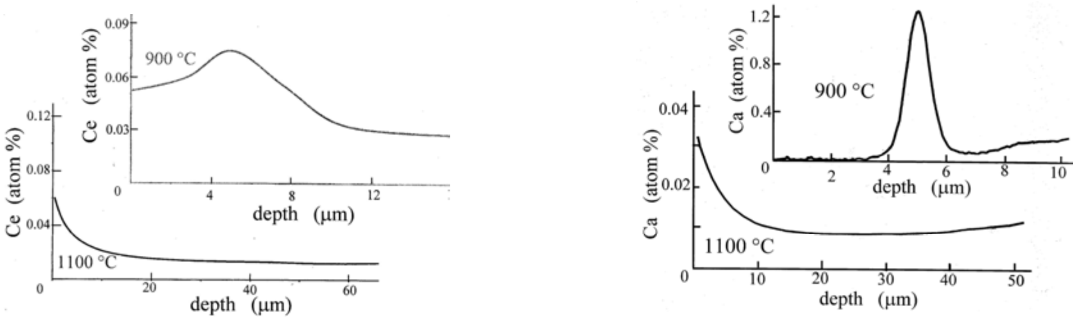

Figure 6 EPMA concentration-depth profiles in oxide films, after 18h of oxidation, at 900°C and 1100°C. (metal/oxide interface taken as initial position of analysis)

At higher temperatures and in thicker scales, Ca^{2+} or Ce^{4+} become progressively more dilute in the oxide films. At 1100°C for instance (Fig.6), their amount is very low and it shows only a weak increase close to the metal surface, which corresponds to the equilibrium segregation [1].

4 Transport properties of pure and Ca (or Ce)-doped $Ni_{1-x}O$ single crystals

4.1 *Electrical conductivity at thermodynamical equilibrium*

One can recall that the prevailing defects in $Ni_{1-x}O$ are electron holes (h°) and α time ionized cationic vacancies ($V_M^{\alpha'}$), whose concentrations depend of both temperature (T) and oxygen partial pressure (P_{O2}) [1-3]. Information concerning these defects can be obtained from electrical conductivity (σ) measurements:

$$\sigma = e\mu p = \sigma_o (P_{O2})^{1/2(\alpha+1)} \exp (1/RT) [(-\Delta H_{\mu}-\Delta H_v)/(1+\alpha)] \quad . \square$$

where e is the charge of the electron, p the hole concentration per cm^3, μ the hole mobility ($\mu=\mu_o \exp -\Delta H_{\square}/RT$), ΔH_{μ} the hole enthalpy of mobility

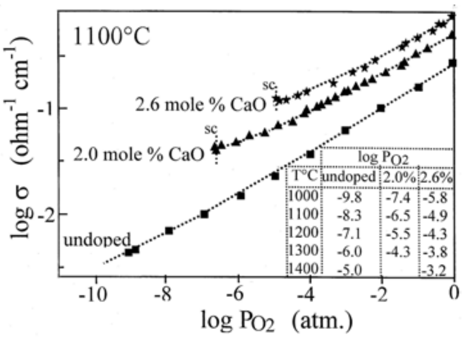

	log P_{O2}		
T°C	undoped	2.0%	2.6%
1000	-9.8	-7.4	-5.8
1100	-8.3	-6.5	-4.9
1200	-7.1	-5.5	-4.3
1300	-6.0	-4.3	-3.8
1400	-5.0		-3.2

Figure 6 Influence of the calcium amount on the electrical Cconductivity of $Ni_{1-x}O$, at 1100°C.

The dissociation pressure of undoped and Ca-doped $Ni_{1-x}O$ single crystals is reported in the Table, between 1000° and 1400°C.

In Fig.6, we have reported the electrical conductivity values obtained at 1100°C, with single crystals doped with 2.0 and 2.6 mole % CaO, as a function of log P_{O2}. These results show a short-circuit (sc) at low P_{O2}, indicating the precipitation of a metallic phase. The P_{O2} values, corresponding to the short circuits observed between 1000° and 1400°C (Fig 6 /Table), show a shift of the Ni/NiO phase boundary to higher P_{O2}, which increases with the calcium amount..

4.2 *Electrical conductivity in transient state.*

According to Fick law, the flux of defects which appears in a crystal in the presence of a defect concentration gradient (dC_d/dz), may be written in the z direction [1-3]:

$$J_V = -\tilde{D} \, (dC_d/dz) \quad (4)$$

where $\tilde{D} = (1+\alpha) D_V$ is the chemical diffusion coefficient and D_V the diffusion coefficient of the α time ionized cationic vacancies.

It should be pointed out that $\tilde{D}$ allows to know the time to reach the new oxide equilibrium conditions or the metal oxidation kinetics.

The chemical diffusion coefficient values (D_{chim}) were determined from experiments in which the electrical conductivity was measured as a function of time, following a sudden change of the external P_{O2} [1,2]. The Arrhenius plot of $\tilde{D}$ for undoped and Ca-doped $Ni_{1-x}O$ single crystals are reported in Fig.7. These results show that Ca additions increase the oxidation or reduction kinetics of the single crystals, in their stability range, due to the increase of the vacancy diffusion coefficient:

$$D_V(\text{Ca-doped NiO}) >> D_V(\text{undoped NiO}) \quad (5)$$

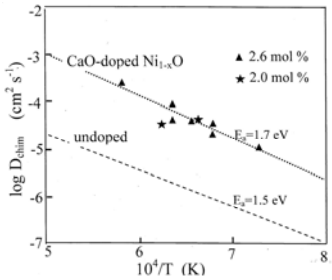

Figure 7 Chemical diffusion coefficient of undoped and Ca-doped $Ni_{1-x}O$ single crystals [1].

The re-equilibration oxidation kinetics of an undoped and a Ce-doped $Ni_{1-x}O$ single crystal, at 1000°C, are reported in Fig.8. These results show that Ce^{4+} leads to a decrease of the oxidation kinetics, i.e of $\tilde{D}$

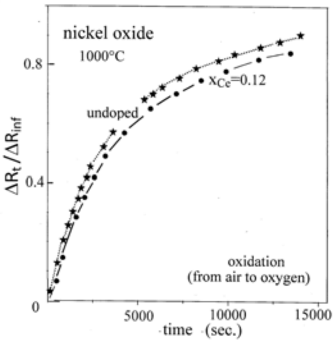

Figure 8 Re-equilibration kinetic of a Ce-doped Ni_1-xO single crystal, at 1000°C

4.3 *Kinetic demixing experiments*

Kinetic demixing processes occur in multi-component oxides in presence of an external driving force ($\mathfrak{F}$), due to an oxygen chemical potential gradient ($\mathfrak{F}=d\ln a_O/dz$), as in oxidation layers (Fig.6), or to an applied electrical field E ($\mathfrak{F}=q_iE/kT$), for instance.

The cationic fluxes in p-type semi conducting oxides can then be described, if one neglects correlation effects [1,2], by the following expression:

$$J_i = C_M D_i[-(dx_i/dz) + x_i\ \mathfrak{F}] \quad (6)$$

with $\mathfrak{F} = 1/2\ d\log(P_{O2})/dz = (1 + \alpha)(d\ln[V^{\alpha}]/dz)$, (7) In these expressions, C_M is the overall concentration (in mol/cm^3) of cationic sites in the lattice, x_i the mole fraction of cations i, dx_i /dz their concentration gradient, D_i their diffusion coefficient, $a_O=(P_{O2})^{1/2}$ and dln[V^{α}]/dz the vacancy concentration gradient

In Fig.9 we have reported the results of a kinetic demixing experiment performed under flowing air, at 1292°C. The EPMA analysis at the end of the experiment shows an enrichment of calcium near the cathode. Therefore, it follows from Eqs.6,7:

$$D_{Ca}>D_{Ni} \qquad (8)$$

This result, in agreement with the enrichment of calcium in the outer oxidation layer, at 900°C (Fig.6), confirms that cation redistribution in the scale is due to a kinetic demixing process.

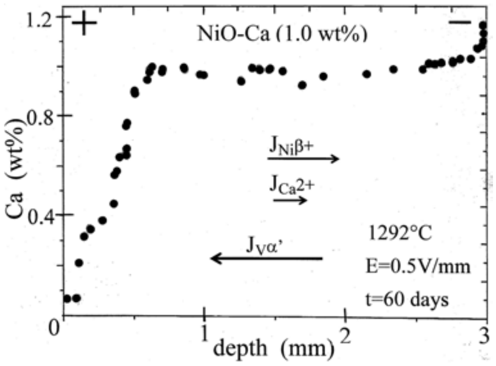

Figure 9 Kinetic demixing profile through an initially homogeneous Ca-doped $Ni_{1-x}O$ single crystal maintained in air under 0.5 V/mm, for 60 days, at 1292°C.

5. *Discussion*

The set of data reported previously shows that the growth of nickel oxide layers is controlled by the outward cation grain boundary diffusion, at T<1200°C.

For CeO_2 coated specimens, these results are in agreement with re-equilibration kinetics of Ce-doped Ni_1-xO single crystals (i.e. with $\tilde{D}$). The decrease can then be explained both by a decrease of the cationic vacancy diffusion coefficient (D_V) and by CeO_2 precipitates near the original metal surface (Fig.6), which lead to diffusion blocking effects, all the more important that the temperature is low..

For CaO coated specimens, a reduction of the oxidation kinetics is observed, at T<1200°C. These results are in discrepancy with the values of $\tilde{D}$ in single crystals. On the other hand, blocking effects, ascribed to CaO precipitates at grain boundary, have been invoked [5]. This assumption is in conflict with the growing of the oxide layers by a diffusion process. Therefore, according to the previous results, it appears that the beneficial effect of CaO coatings can be explained:

- First, by the EPMA analysis, which reveals calcium concentrations higher than the limit of solubility, at 900°C (Fig.6), near the original metal surface, as previously shown for cerium.
- Second, by the expression which describes the transport processes of the cationic species (Eqs.6,7) and which predicts that the cationic fluxes depend of two term: $\mathfrak{F}$ and D_i.

-Concerning the driving force of diffusion $\mathfrak{F}$ (Eq.7/ $\mathfrak{F} = 1/2 \; d\log(P_{O2})/dz$), it depends of the oxygen partial pressure gradient across the scale. The shift of the $Ni/Ni_{1-x}O$ phase boundary to higher P_{O2} leads then to a decrease of $\mathfrak{F}$ and therefore of the oxidation kinetics all the more important that the calcium amount is high (Table/Fig.6).

-Concerning the grain boundary diffusion coefficient D_i, it is difficult to conclude since this diffusion coefficient is characteristic of a specimen with a given microstructure.

6. Conclusion

Finally, this study has allowed us to show that oxidation of CaO or CeO_2–coated nickel polycrystals, at T<1200°C, is controlled by the outward diffusion of cations at grain boundaries and by the presence of CaO or CeO_2 precipitates near the initial surface position, leading to diffusion blocking effects all the more important that the temperature is low. For the CeO_2–coated specimens, the decrease of the oxidation kinetics is also due to the decrease of the vacancy diffusion coefficient through the oxide scale, which depends nevertheless of the amount of Ce^{4+} in the layer. For the CaO coatings, it results of the decrease of the driving force of diffusion ($\mathfrak{F}$), due to the shift of the Ni/NiO phase boundary to higher P_{O2}, which increases with the calcium amount.

Furthermore, in agreement with previous experimental findings, the decrease of the vacancy fluxes which arrive at the interface oxide/ nickel explains the improvement of the scale adhesion to the substrate observed in coated specimens.

References

1. H.Aïdrous, L.Cieniek, N.Halem, J.Kusinski, C.Petot, G.Petot Ervas, *Sol.St Ionics,* 261 (2014) 117-124
2. N.Halem, M.Abrudeanu, G.Petot Ervas, *Mat. Sci. and Eng. B*, 176, 1002-1009 (2011)
3. P.Kofstad, Nonstoichiometry, *Diffusion and Electrical Conductivity in Binary Oxides*, Wiley Interscience (1972), *High Temperature Corrosion*, Elsevier Applied Science (1988).
4. A.Atkinson, *Review of Modern Physics,* 57,2 (1985) 437-470
5. .J.Gonzalez Thesis N°1050, Institut National Polytechnique, Toulouse (1995).